F. M. Burdekin, H. K. Saket*, S. D. Thurlbeck*, and J. G. Frodin**

Aspects of Assessment of Defects in Welded Joints and Related Reliability Analysis Treatments

REFERENCE Burdekin, F. M., Saket, H. K., Thurlbeck, S. D., and Frodin, J. G., **Aspects of assessment of defects in welded joints and related reliability analysis treatments**, *Defect Assessment in Components – Fundamentals and Applications*, ESIS/EGF9 (Edited by J. G. Blauel and K.-H. Schwalbe) 1991, Mechanical Engineering Publications, London, pp. 1051–1071.

ABSTRACT After a brief review of the proposed revisions to BSI Document PD6493, examples are given of results of stress intensity factors for fillet welded joints at both the root and the toe of the weld. These results are then extended to the cases of rectangular and tubular joints to give magnification factors to allow for local bending of the tube walls. Three dimensional elastic–plastic finite element analysis results are reported on work to determine ultimate collapse strength of tubular joints. Experimental model tests on tubular joints confirm that cracks up to about 20 percent of the circumference have little effect on plastic collapse, although their effect on fracture depends on absolute crack size and fracture toughness. Progress on allowing for variability/uncertainty in input data on reliability is briefly described.

Notation

a	Half crack length for through thickness defect, half crack height for embedded cracks, crack height for surface defects
b	Brace width for SHS
B	Chord width for SHS
d	Brace diameter of CHS
D	Chord diameter of CHS
E	Modulus of elasticity
J	J integral
K	Stress intensity factor
l	Fillet weld leg length
L	Surface attachment length, distance between fillet weld toes
M_k	Magnification factor on K
P	Load
p, q	Parameters in expression for M_k
R	Weld toe radius
S_r	Collapse load ratio based on flow strength
t	Brace thickness
T	Chord thickness
W	Gross cross section width
β	Ratio d/D
δ	Crack tip opening displacement

* UMIST, PO Box 88, Manchester, M60 1QD, UK.

σ Stress
θ Weld toe angle
γ Partial safety factor

Subscripts
fe Finite element result
g Magnification effect in SHS members
r Ratio of applied to resistance parameter
y Yield
1 Opening mode

Introduction

There are various complexities in the assessment of defects in welded joints which are often overlooked by the fracture mechanics specialists, but which can have a significant influence on overall assessment. In particular welded joints are often associated with stress concentrations arising from the load path through the connection, or with local stress concentrations inherent to the weld geometry itself. In addition, welded joints inevitably have some level of residual stress associated with them, which in the as-welded condition may be up to the yield strength of the weld metal. Finally, the mechanical properties, both strength and toughness, of the weld metal may be significantly different from parent material, and these differences may have a significant influence on assessment of defects. Very often the scatter and uncertainty of material properties is greater for welded joints than it is for parent material and this in turn leads to problems in defect assessment.

When these complications are taken together with practical thicknesses and toughness levels for structural weldments, it is found that linear elastic fracture mechanics is no longer adequate, and elastic–plastic fracture mechanics assessments must be adopted. Two of the earliest and most widely used formalised methods of defect assessment are the BSI PD6493 : 1980 approach (**1**) and the CEGB R6 approach (**2**).

The PD6493 approach required separate checks on fracture using either LEFM or the CTOD design curve as appropriate, and plastic collapse based on net section yielding whereas the CEGB R6 assessment diagram automatically builds in a check against plastic collapse and fracture at the same time. It is important to recognise that the R6 assessment diagram fracture axis is the ratio of applied stress intensity factor to fracture toughness, and that this is an elastic parameter. The effect of plasticity is taken into account in the shape of the assessment diagram, so that as the net section stress increases towards the yield strength, the total crack driving force is increased by plasticity, and the permissible elastic proportion of this reduces. This is shown in Fig. 1 on the R6 Rev. 2 assessment diagram where the height of the diagram at any value of S_r is the permitted elastic parameter K_r, whereas the shaded area above the diagram represents the enhancement of the crack driving force due to plasticity, assumed to reach the same critical value of real fracture toughness for failure.

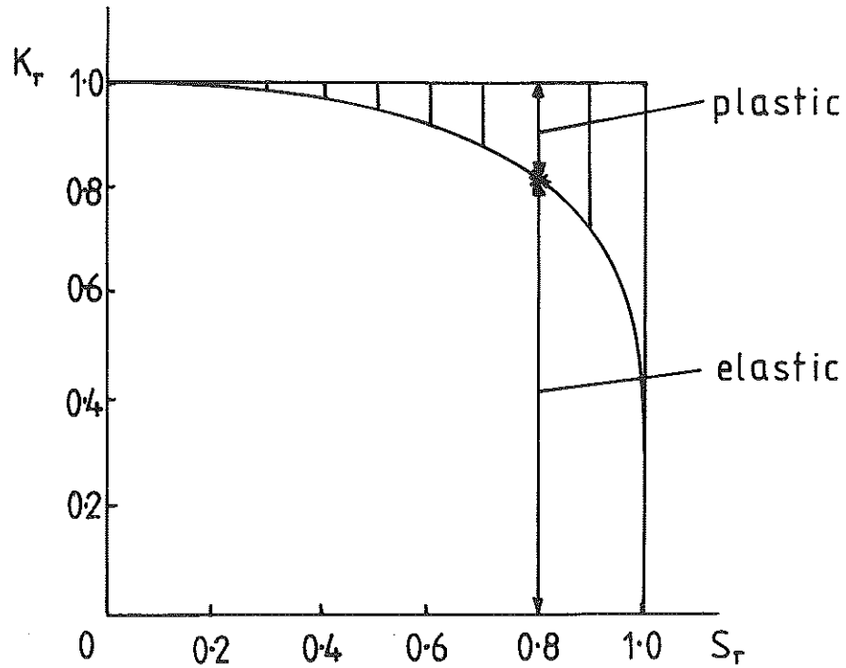

Fig 1 R6 Rev. 2 assessment diagram showing plastic enhancement of crack driving force

It is therefore to be expected that the shape of an assessment diagram of this kind ought to be dependent both on material stress/strain curve and on geometry. This is indeed the case, and the CEGB R6 Rev. 3 document (**3**) is based on different forms of assessment diagram for different materials, the curves being a lower bound for geometries and loadings commonly encountered.

Revisions to BSI document PD6493

The 1980 version of PD6493 has served industry well in providing a basis for making rational judgements on the significance of defects on a fitness for purpose basis. Inevitably with developing research work, improved assessment methods have now become available, and for the last two or three years deliberations have been in progress on revisions to PD6493 (**5**). It is anticipated that the revised proposals will be issued sometime in 1990. The Committee charged with the task of executing these revisions has tried to bring together the best parts of PD6493 and CEGB R6 approaches in the revised version and to make these approaches compatible.

The revised PD6493 document will offer the opportunity of assessment at three alternative levels of complexity and accuracy. The three assessment diagrams for the levels concerned are shown in Fig. 2.

For the level 1 procedure, stress concentrations, residual stresses, and stress gradients are all treated as having a uniform stress value equal to the maximum tensile stress present. The assessment diagram builds in a safety factor of 0.7 on toughness and 0.8 on plastic collapse as shown by the level 1 box in Fig. 2. If it is found by carrying out a simple screening assessment using these assumptions that defects are acceptable, no further assessment is necessary.

The level 2 procedure is intended to represent an accurate assessment, in which as accurate an assessment of driving force parameters is made as possible. At all three levels, the assessment can be made via a stress intensity factor route or a crack opening displacement route, depending on the form of fracture toughness data available. It is important to note however that where crack opening displacement methods are used, the ordinate axis of the assessment diagram is $\sqrt{\delta_r}$, where δ_r is the ratio of *elastic* crack opening displacement driving force to fracture toughness. The required δ_1 is calculated directly from the stress intensity factor K_1 by the relationship $K_1^2 = E\sigma_Y \delta_1$.

The level 3 approach in the revisions to PD6493 uses the R6 Rev. 3 option 1 assessment diagram. It is intended in PD6493 that this approach should only be necessary either for high strain hardening materials, or for a tearing analysis, and in other respects the procedures are the same as the level 2 approach.

Finally, it should be pointed out that the revised PD6493 level 2 assessment diagram (corresponding to R6 Rev. 2) is really based on an elastic perfectly

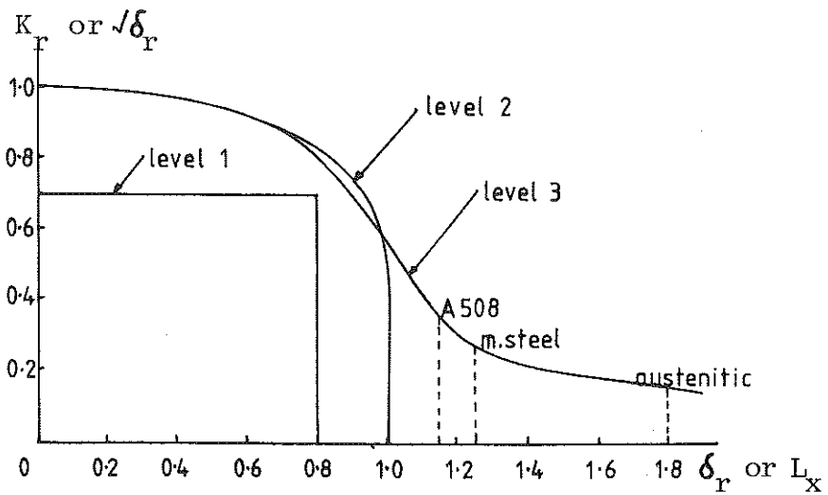

Fig 2 Revised PD6493 assessment diagrams

plastic material with a flow strength equal to the average of yield and ultimate strengths. The need for the R6 Rev. 3 approach (and revised PD6493 level 3) arises from the effect of the stress/strain curve on the assessment diagram when significant strain hardening occurs. It is particularly important in the context of assessment of defects in welded joints to note that weld metals usually have a very high yield to ultimate strength ratio. Thus for assessment of defects located in weld metals with such stress strain curves, the level 2 assessment diagram should be satisfactory.

Assessment of fillet welded joints

Very often, little attention is given to assessment of fillet welded joints other than fatigue assessments of inherent design behaviour. It is necessary to consider separately the effect of weld root defects growing in the weld itself, and weld toe defects growing into the parent material.

Root defects

Generally speaking the strength of fillet welds is taken as being dependent on the weld throat dimension, and basic design procedures for fillet welds usually only consider this aspect. Thus the required design size for a fillet weld is found by combining the loadings in different directions to give an effective stress on the weld throat, and setting this to a permissible stress dependent upon the type of Code procedure (allowable stress or limit state). Thus, no real consideration is given to risks of fracture or to considerations of toughness requirements for fillet welds.

The assessment diagram approach of the CEGB R6 and revised PD6493 procedures allows assessment to be carried out by consideration of linear elastic stress intensity factors, and plastic collapse behaviour separately. The plastic collapse behaviour of fillet welds is reasonably well established, but to use the assessment diagrams, stress intensity factor solutions are also required. The only published work available on stress intensity factors for the root region of fillet welds appears to be that of Frank and Fisher (6) carried out some years ago and leading to rather complex equations. A separate investigation has now been carried out by Saket (7) using the ABAQUS three-dimensional elastic–plastic finite element program to determine the ratio of stress intensity factor for the crack like defect forming the unfused region between fillet welds and the applied tensile stress to the stem plate connected by the fillet welds. This arrangement is shown in Fig. 3 together with a typical finite element mesh using crack tip elements to determine the stress intensity factor values. An average of 250, 8-noded bi-quadratic, reduce integration plane strain elements were used in each mesh analysed. It was found that the results could be fitted by a relatively simple expression, (Fig. 4) shown as equation (1) over the ratio of a/W of 0.25 to 0.45, where a is the half crack size, and

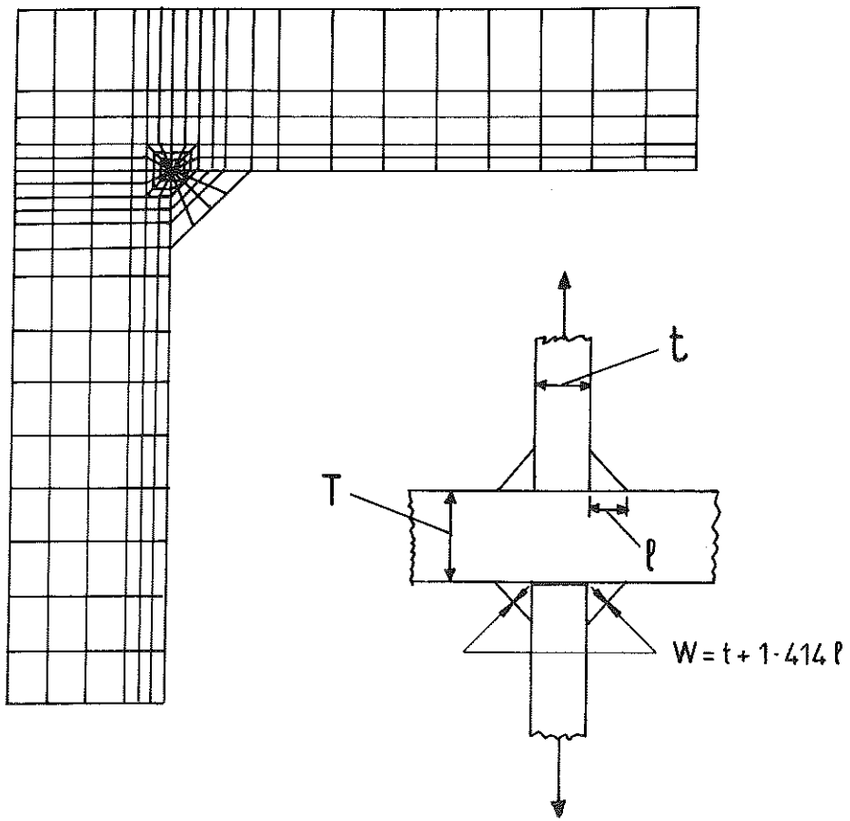

Fig 3 Typical finite element mesh for cruciform fillet welded joints

W is the effective width of the joint, taken as attachment thickness plus both weld throats (equation (2)).

$$\frac{K_{fe}}{K_{tan}} = 2.88\left(\frac{a}{W}\right) - 0.074 \tag{1}$$

where

$$K_{tan} = \sigma_{plate}\sqrt{\left(W \tan \frac{\pi a}{W}\right)}$$

$$W = t + 1.414l \tag{2}$$

These equations enable the elastic stress intensity factor to be calculated for the root of different fillet weld situations, and provided fracture toughness information is available on fillet welds at the relevant temperature, the parameter K_r can then be calculated. The plastic collapse parameter S_r should be

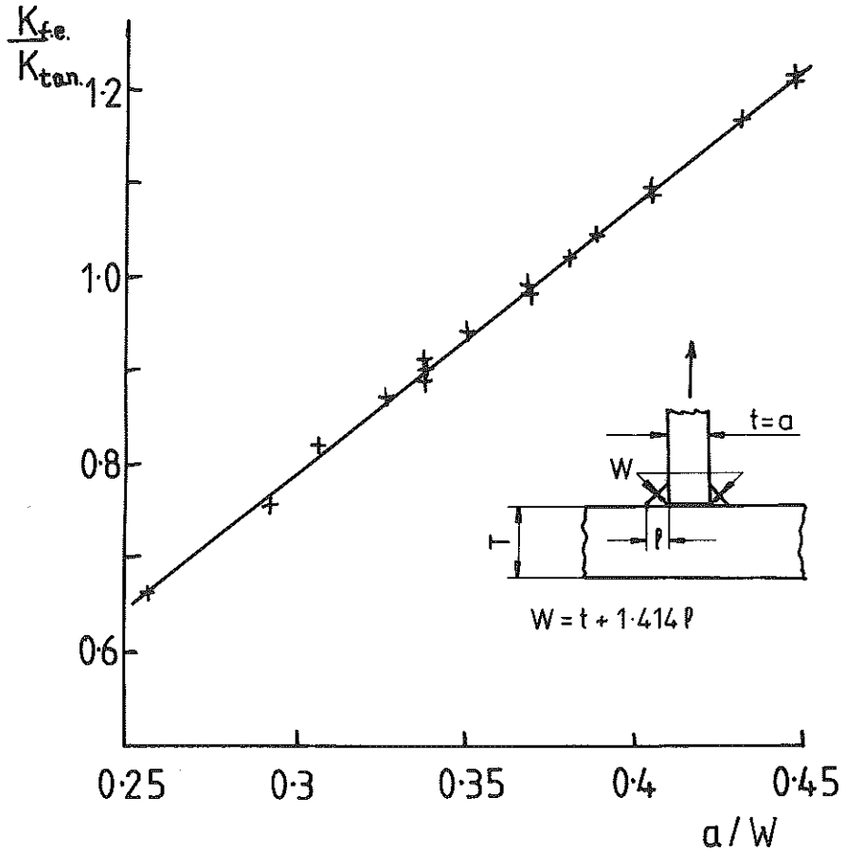

Fig 4 Normalised stress intensity factors for fillet weld root

calculated directly from the equivalent stress on the net section weld throat using a von Mises yielding criterion.

Weld toe defects

Cracks growing at the toe of a fillet weld detail are subject to a stress concentration effect, which is best represented by the magnification factor M_k first introduced by Maddox **(8)**. There has been considerable work at The Welding Institue and at UMIST into determination of parametric equations for M_k factors. The Welding Institute work is based mainly on cruciform joints, and is the basis of that included in the revision to PD6493. The UMIST work originated with that of Ahmet **(9)** and Lie **(10)**, and it was this work that showed that the effect of different attachment thicknesses and weld sizes could be rationalised in terms of the ratio of total surface attachment length to plate thickness (L/T).

The more recent work at UMIST has been as part of the MTD Ltd. Defect Assessment Programme for Offshore Tubular Structures in determining M_k factors for plate 'T' joints with different values of L/T, weld angle, θ, and weld toe radius, R. The basic approach is to carry out finite element analysis of the relevant models of uncracked two-dimensional geometries, to determine the stress distribution on the required crack propagation plane, and then to use Albrecht's method **(11)** to determine the stress intensity factor. This is converted to an M_k factor using standard edge crack solutions for the same depth of crack without the attachment stress concentration present.

Typical results for M_k plotted against the ratio of crack depth at the weld toe to thickness are shown in Figs 5, 6, and 7 showing the effect of each of the main variables on M_k. The general result of both The Welding Institute and UMIST analyses is that M_k can be expressed approximately in the simple expression of equation (3) as a function of a/T.

$$M_k = p\left(\frac{a}{T}\right)^q \tag{3}$$

where p and q are constants over discrete zones of a/T dependent on the other geometry variables, and on the proportion of bending in the loading. Some selected examples of values of p and q are given in the Appendix.

As far as assessment of defects at weld toes is concerned, the M_k factors permit calculation of stress intensity factors, and hence the K_r ratio on the assessment diagram provided fracture toughness values are known. The collapse ratio parameter S_r should not be significantly affected by the stress concentration of the surface attachment for cracks at weld toes, and can be determined on the basis of standard solutions for the crack treated as a surface defect extending into the main plate thickness. Given these standard results, the assessment diagram procedures can then be applied to defects at weld toes.

Application to tubular joints

Very little attention has been given to fracture mechanics treatments for square/rectangular sections with fillet welds, or to ultimate strength of circular tubular sections containing crack-like defects. The ultimate strength work on rectangular sections has also been confined generally to uncracked connections. It will be recalled that the assessment diagram approach requires consideration of stress intensity factors or crack opening displacements, and of the ultimate collapse load of the cracked net section.

Square sections

Part of the UMIST research programme of behaviour of welded joints has looked at determination of stress intensity factors at the root of fillet welds in square hollow section 'T' joint connections **(7)**. The SHS geometry and finite

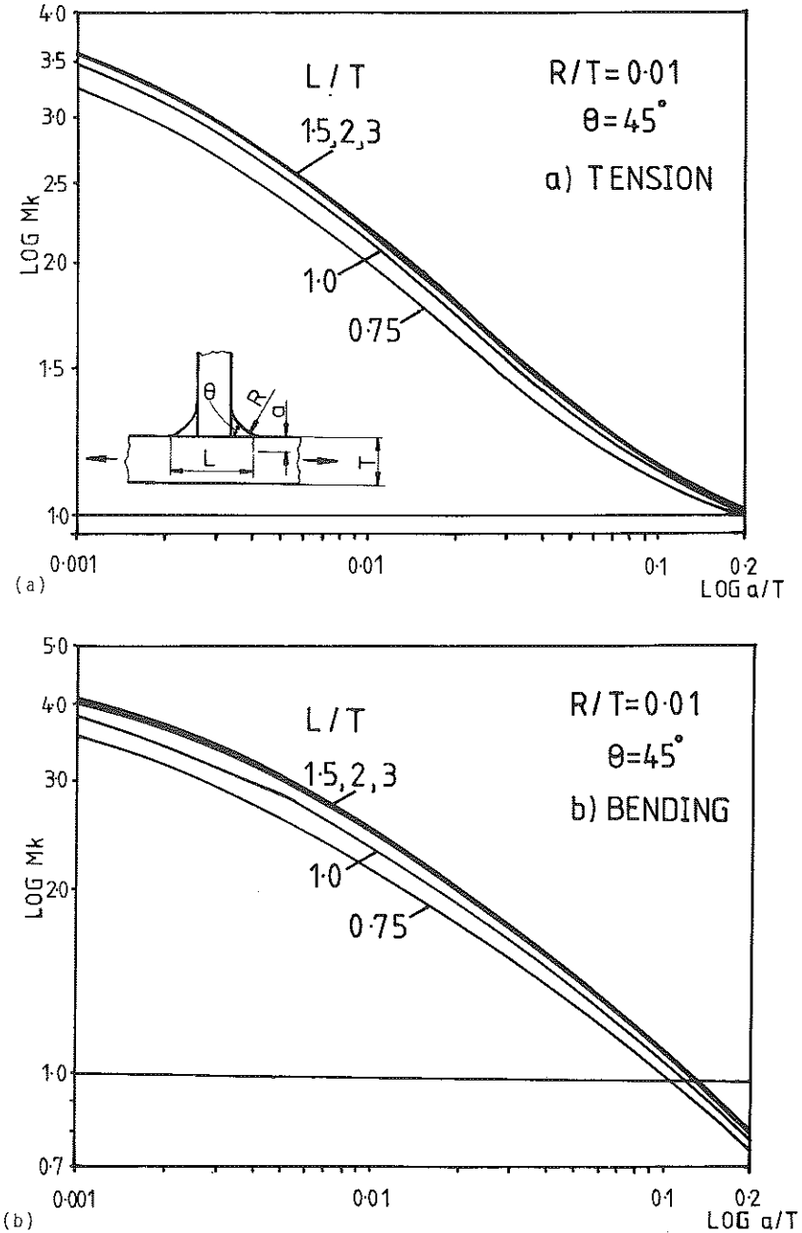

Fig 5 Log M_k against log a/T for varying L/T in (a) tension and (b) pure bending

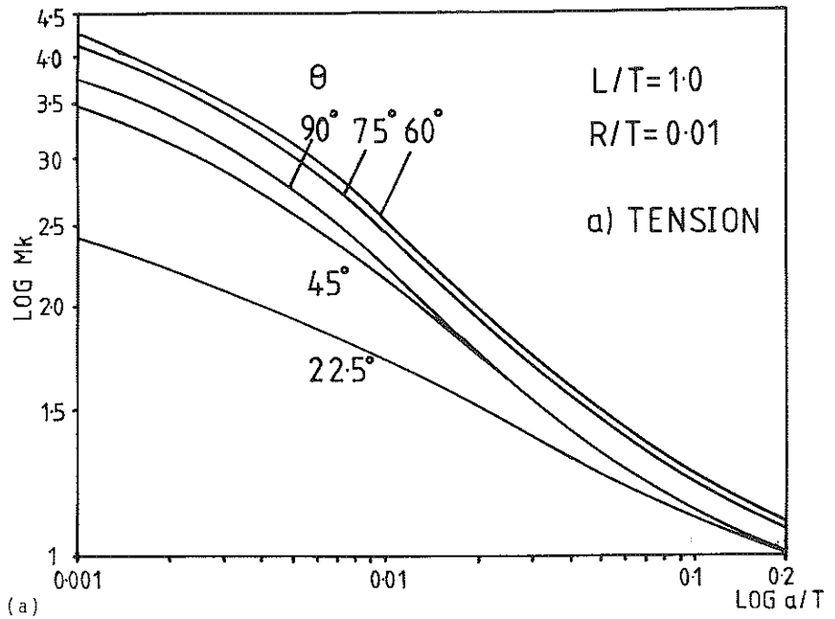

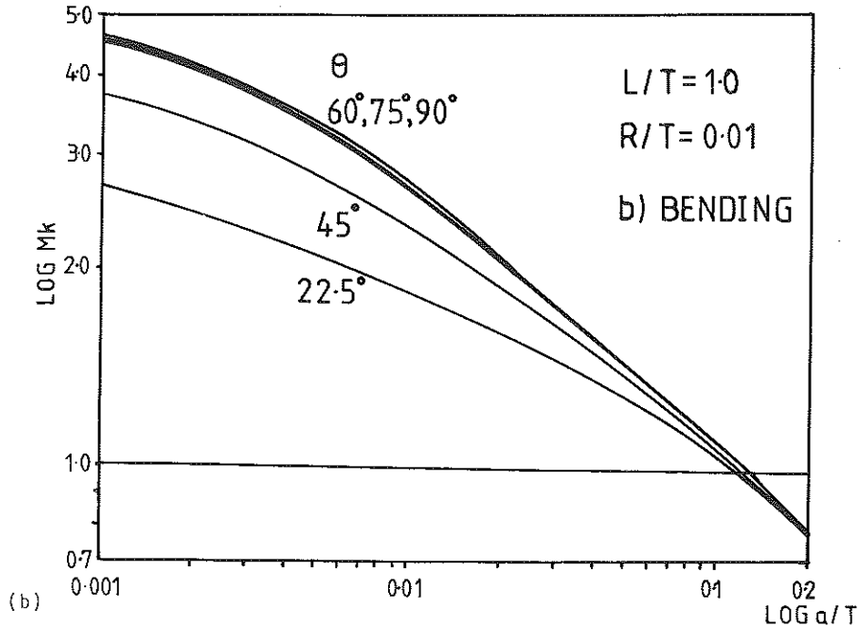

Fig 6 Log M_k against log a/T for varying weld angle θ in (a) tension and (b) pure bending

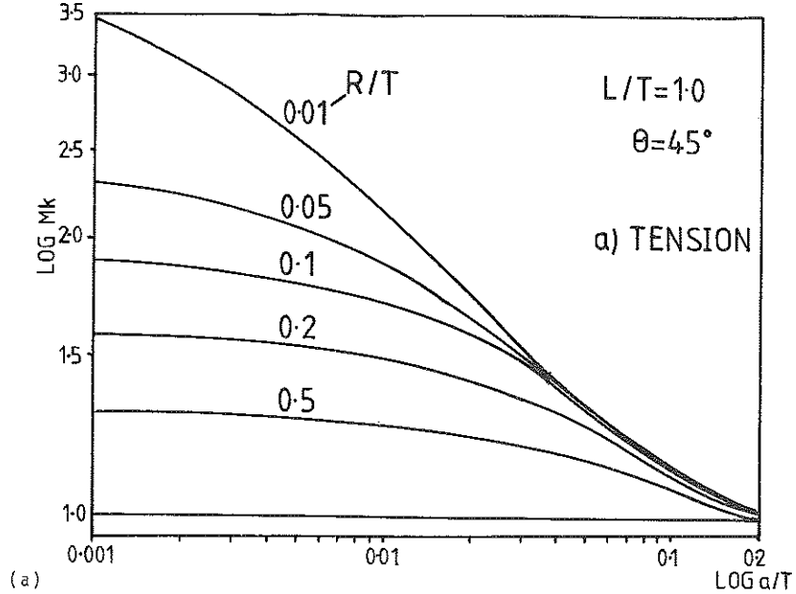

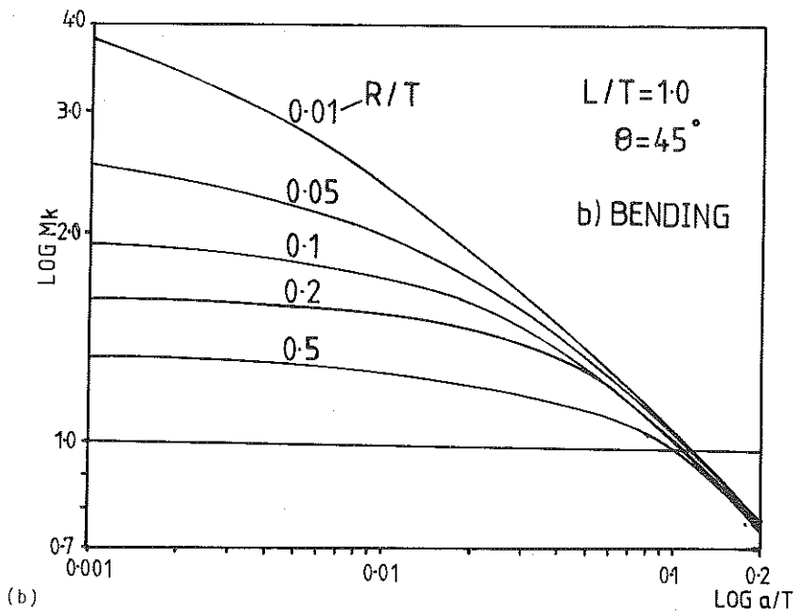

Fig 7 Log M_k against log a/T for varying R/T in (a) tension and (b) pure bending

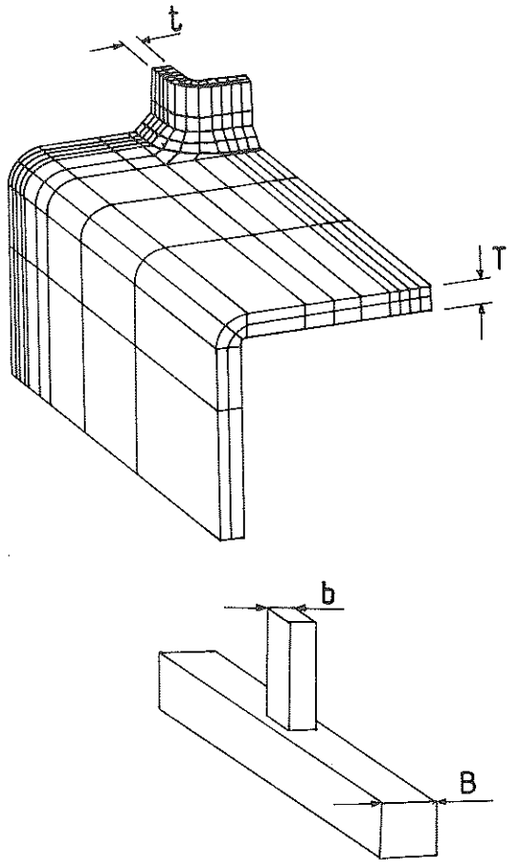

Fig 8 Typical finite element model of SHS joint

element representation of it are shown in Fig. 8. In these types of joint, the flexibility of the walls of the rectangular members leads to additional bending stresses developing which depend upon the ratio of tube sizes connected. The geometries analysed have b/B ratios varying from 0.25 to 0.67, t/T ratios from 0.5 to 1.0, and variations in fillet weld leg length to brace thickness from 0.5 to 1.0. The finite element models analysed one-quarter of a cruciform joint taking advantage of symmetry, and each mesh consisted of 860 brick elements. A cluster of crack tip elements was used at the root of the fillet weld around the perimeter of the joints modelled. In all the meshes analysed, J integral values were computed at 25 positions along the crack front from the middle of the side wall to the middle of the cross wall. These J integral values were evaluated for three contours surrounding the crack tips, with the material behaviour restricted to linear elastic. These J values were then converted to

equivalent stress intensity factor values and compared to the corresponding results for the two-dimensional plate fillet weld only case. An example of these results showing the variation of stress intensity factor at the root of the fillet weld around the perimeter for different geometries is given in Fig. 9. The peak stress intensity factor around the perimeter was taken for each joint geometry, and a magnification factor M_g determined as a multiplier of the two-dimensional finite element fillet weld root results reported previously. The overall results for this magnification factor plotted against the geometric ratio b/B are shown in Fig. 10.

These results, taken with basic fillet weld strength values offer the opportunity of determining fracture toughness requirements/defect size assessments for fillet welds in structural hollow section connections.

Circular sections

In offshore tubular joint construction, the normal practice is for tubular joints to be specified as full penetration butt welds except for very acute angles of intersection where access prevents an adequate preparation. Fillet welded construction of circular sections is used for thin walled CHS members in roof trusses and cranes, and the approach described above for SHS sections can be adopted for assessing the fillet weld itself. As far as failure from the weld toe is concerned, in either circular or rectangular sections, it is now common practice for fatigue design to determine a hot spot stress concentration factor due to local bending of the wall of the tubular member and apply this stress concentration factor in design. It is, however, possible to investigate the effect of

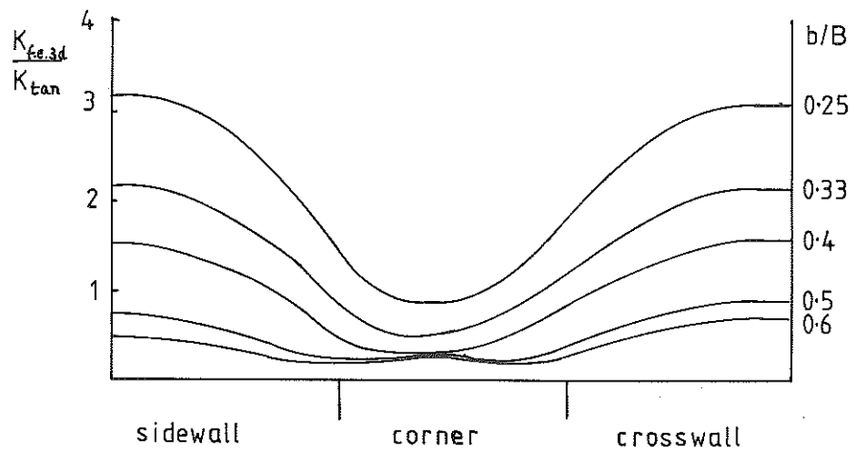

Fig 9 Variation of stress intensity factor at weld root around perimeter of SHS joints

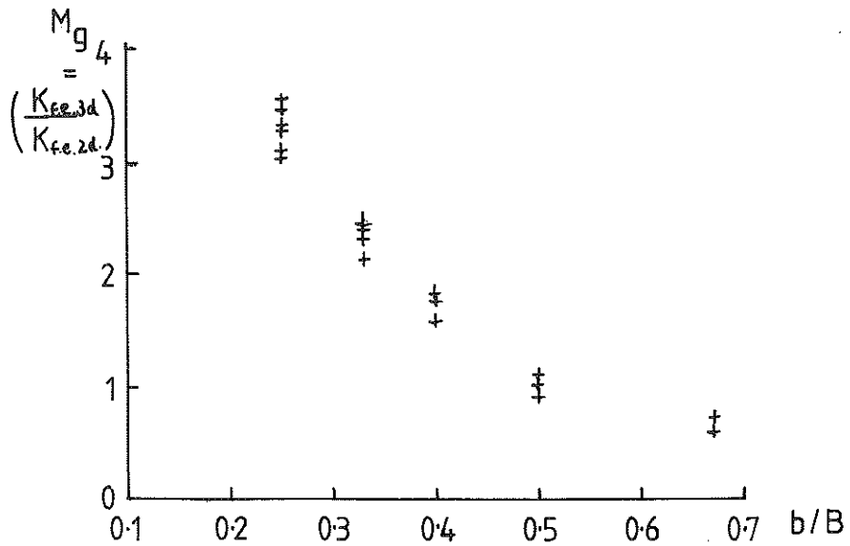

Fig 10 Magnification of stress intensity factors at fillet weld root due to SHS geometry

geometric variables more extensively using finite element and fracture mechanics approaches as attempted, for example, in the work at UMIST **(12)(13)**. The factors required to carry out an assessment of fracture or fatigue for cracks at weld toes are as follows:

(i) the hot spot SCF for the joint geometry;
(ii) the proportion of bending to total stress in the chord;
(iii) the ratio of surface attachment length to chord thickness (L/T);
(iv) the weld angle θ, and weld toe radius, R;
(v) assumed initial and final flaw sizes.

Given the above information, and the applied stress levels, the stress intensity factor can be calculated for cracks at the toes of welds in tubular joints, thus providing the input for the ordinate axis of the assessment diagram.

A separate programme of work has been in progress at UMIST to determine ultimate strength behaviour of circular tubular joints, both in the uncracked and cracked condition. Three dimensional elastic–plastic finite element analyses were carried out on three tubular 'T' joints loaded in axial tension for which data was available from the literature, and for three cruciform tubular joint geometries on which experimental work was carried out as part of the same programme. In each case, ABAQUS shell elements were used in a relatively coarse mesh with no attempt to model the crack tip in detail. This type of element is a reduced integration, 8-noded isoparametric element, and although the non-linear geometry version of the analysis was used it must be accepted that errors will occur at large plastic strains. The

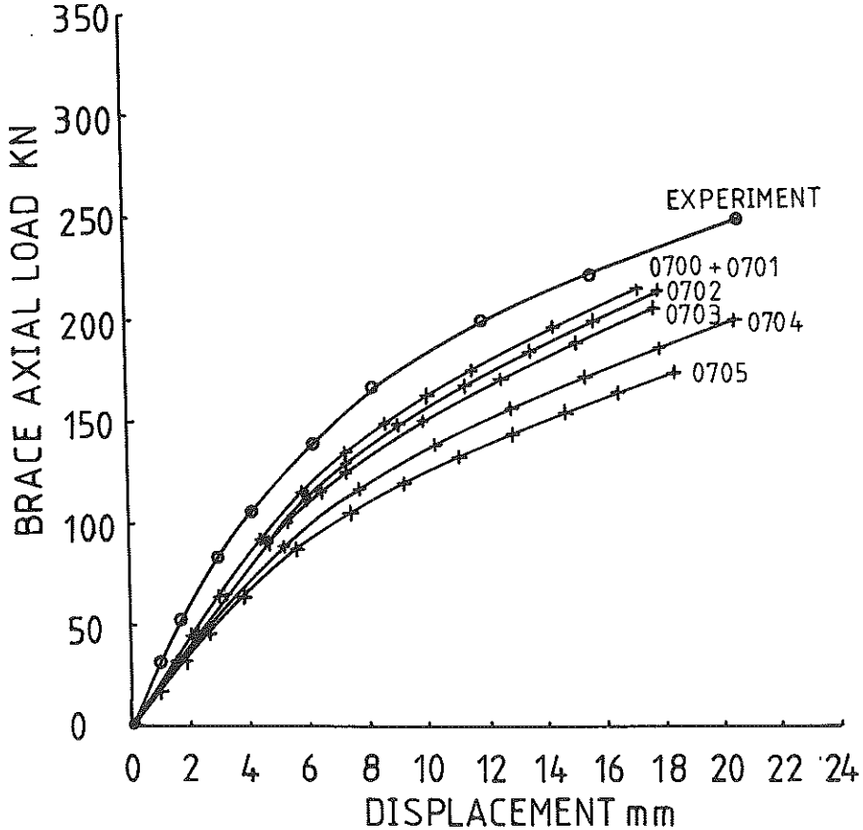

Fig 11 ABAQUS FE predictions of load displacement curves for reference (24), sound + cracked tubular geometry

width of the first row of elements from the weld toe region was selected as about $\sqrt{RT}$, or 5 degrees of arc length around the chord. For each model the first analysis carried out was on an uncracked geometry with the first step as an elastic analysis, followed by load steps allowing plasticity to develop as the load increases. The first analyses were carried out on the geometry reported by Beale and Toprac **(14)** for a 'T' joint with a d/D ratio of 0.3. The material tensile properties assumed were a yield strength of 250 N/mm^2 and a UTS of about 380 N/mm^2 reached at 20 percent strain. It was found that the experimental load displacement curve of Beale and Toprac was reasonably well reproduced, lying between assumptions of fixed and pinned chord ends, with the pinned case overestimating the deflections at a given load. This same geometry of specimen was then reanalysed with through thickness cracks around the weld toe region at the saddle simulated by releasing nodes between elements. Each node released represented a crack length of about 12.5 percent

of the brace/chord intersection, and with the symmetry assumed this represented cracks at both saddle points. The resulting analyses for the load deflection curves are shown in Fig. 11 where the end digit of each model reference number represents the number of nodes released to form cracks. It can be seen that releasing nodes up to 25 percent of the chord intersection length (model 0702) has relatively little effect on the load deflection behaviour and joint stiffness. The results were analysed to determine the area under the load displacement curves, and the complementary area to the load axis, and these areas plotted against the crack length. From these curves values of J were determined as the differential of the area with respect to crack length. An example of the results os such calculations is shown in Fig. 12 for the model geometry tested by Beale and Toprac. From a diagram of this kind the effect of different crack lengths at different toughness levels in reducing the ultimate strength of a cracked tubular joint can be determined. Furthermore the implication of these results is that the ultimate strength for a sound joint is not impaired by the presence of cracks up to a certain minimum size dependent on the fracture toughness.

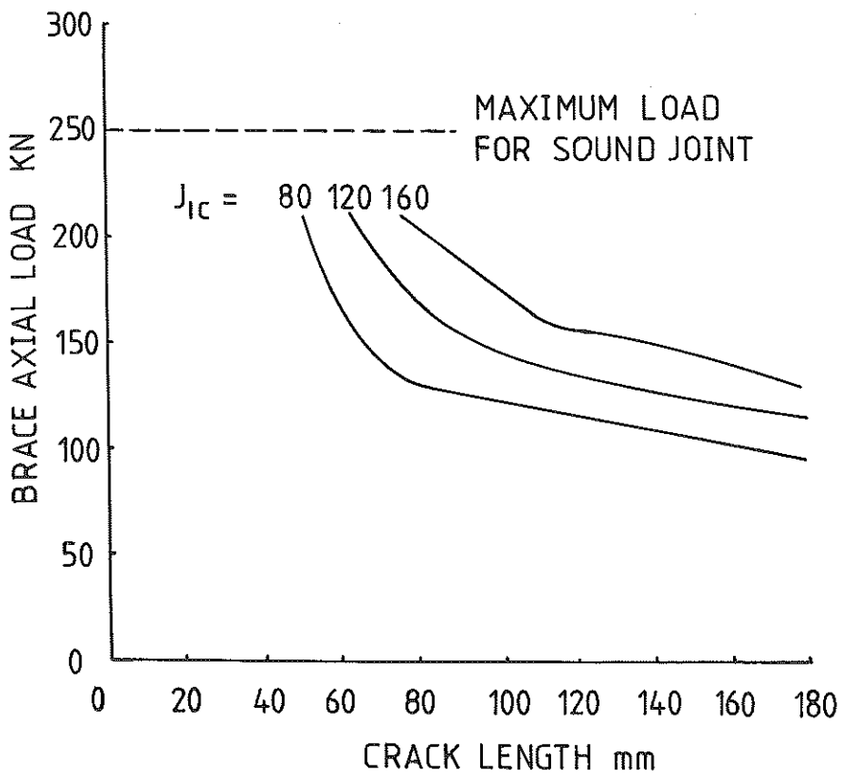

Fig 12 *J* analysis of cracked tubular joints from Fig. 11

To test this situation further, a series of experimental cruciform tubular joint tests was carried out with associated finite element analysis of both uncracked and cracked model geometries. These tests covered a range of d/D values of 0.34, 0.54, and 0.82. For the samples representing different crack lengths laser cuts were made around the toe of the weld to the required length. The results of the experimental tests are shown in Table 1. The ABAQUS calculated load deflection curves for the uncracked and cracked cases of the $d/D = 0.34$ sample are shown in Fig. 13. Again for all the models the finite element analysis predicted very little effect of cracks up to 20 percent of the intersection circumference on the stiffness of the joint, and hence on its load bearing capacity. All the finite element analyses over predicted displacements by some 10 percent compared to experimental values.

The experiments were remarkable in showing a mixture of mode 1 and mode 3 deformation. Figure 14 shows the late stages of model JF3-4 where the brace has pulled out from the chord and a longitudinal shear fracture has started to extend in the chord from the ends of the original laser cut defect.

Returning to the basic question of assessment of defects in such joints, however, the encouraging feature is that the experimental results as shown in Table 1 confirm that up to a certain level of crack length there is no reduction in the *plastic collapse* capacity of tubular joints below that which would be calculated as a basic design strength for an uncracked joint **(15)(16)**. Whilst these results have been obtained on model scale tests, it is clear from both

Table 1 Experimental results on cruciform tubular joints

Specimen		P (*CALC*) (*kN*)	P (*EXP*) (*kN*)	*CL* (*mm*)	*CLR* (%)	*PR* (%)	*PRAB* (%)
$\beta = 0.34$	JF1-1	85.1	96.1	—	—	—	—
$d = 48.3$	JF1-2		97.6	20	12	(1.5)	1.2
$t = 5.0$	JF1-3		*96.9	37	23	(1.0)	7.2
	JF1-4		*85.0	54	33	11.5	14.5
$\beta = 0.54$	JF2-1	117	132	—	—	—	—
$d = 76.1$	JF2-2		121	25	10	8.3	3.2
$t = 5.0$	JF2-3		*118	53	21	10.6	13.0
	JF2-4		*114	80	32	13.6	22.8
$\beta = 0.82$	JF3-1	181	215	—	—	—	—
$d = 114.0$	JF3-2		214	38	10	0.5	4.0
$t = 5.0$	JF3-3		184	79	20	14.4	22.0
	JF3-4		148	130	33	31.2	34.0

* Uncracked branch failed
P (CALC) = Predicted load from UEG equations (kN) ($f_y = 380$ N/mm^2)
P (EXP) = Maximum recorded load (kN)
CL = Original crack length (mm)

$$\text{CLR} = \text{Ratio of } \frac{\text{Crack length}}{\text{Intersection length}} \text{ (percent)}$$

PR = Percentage reduction (increase) of failure load of cracked specimen compared with uncracked specimen
PRAB = Percentage reduction in ABAQUS load at failure displacement

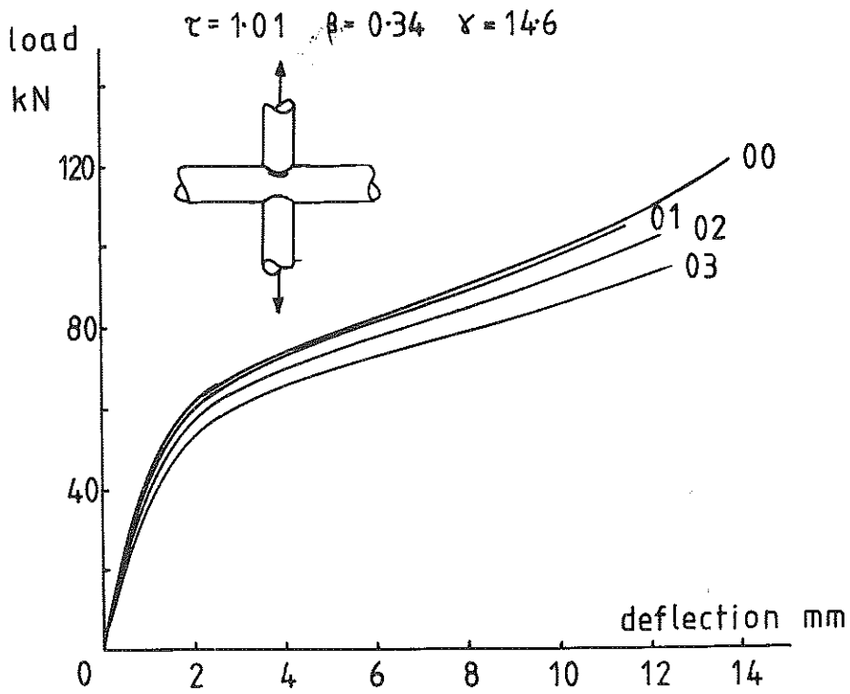

Fig 13 ABAQUS FE predictions of load displacement curves for sound and cracked tubular joints

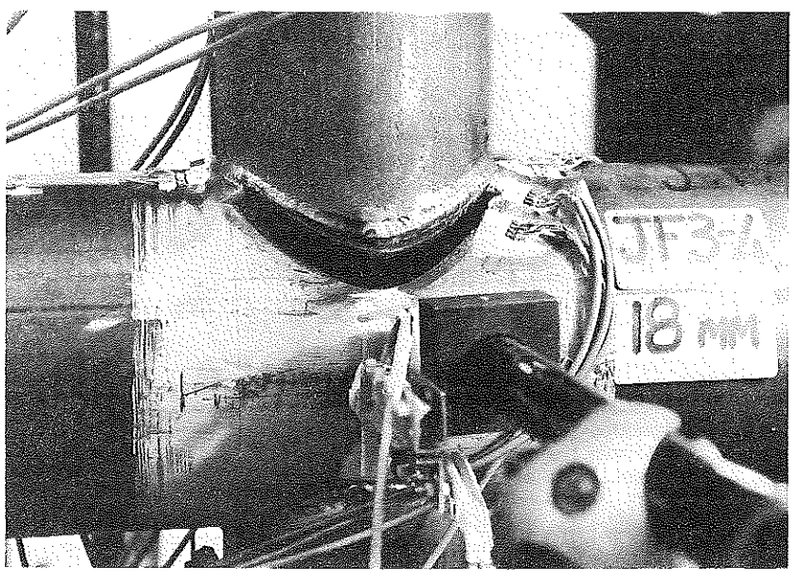

Fig 14 Deformed state of specimen JF3-4 testing showing combination of mode 1 and mode 3 deformation, and mode 3 tearing at ends of initial defect

models and finite element analyses that the scale model behaviour will represent full scale behaviour as far as plastic collapse is concerned. The models will not represent full scale behaviour as far as fracture is concerned and here it is necessary to determine crack driving force parameters to establish the intervention of fracture. It is clearly now possible, however, to return to the assessment diagram approach, at least as far as cracks up to about 20 percent of the circumference of tubular joints are concerned and use the uncracked design strength as the collapse load from which to calculate the S_r values on the assessment diagram.

Reliability aspects

The problem of dealing with uncertainties in the input variables for a fracture mechanics analysis is best dealt with by a combination of probabilistic fracture mechanics and reliability analysis. Again, as part of the MTD Ltd Defect Assessment Programme, work to provide guidance on these aspects has been in progress at Glasgow University and at UMIST (17). The basis of the approach has been use of level 2 reliability analysis methods to determine the reliability index and hence probability of failure for assumed uncertainty/variability in input data. These analyses have shown that scatter in toughness has probably the greatest effect on the resulting reliability but they offer the opportunity of calibrating partial safety factors to be used in the fracture mechanics equations in order that the required reliability is built in.

Such an approach is being offered as an option in the revisions to P6493, the alternative being the assumption of pessimistic values for all of the input data with consequent unknown conservatism. The approach suggested in the PD6493 revisions is a broad consideration of consequences of failure; for example, distinguishing between redundant members where failure would be contained locally, to critical members where failure would be catastrophic for the whole structure. The partial coefficients to be applied to stress, toughness, and defect size depend upon the scatter/variability of this data. Typical values of the coefficients are shown in Table 2 for use with the revised PD6493 level 2 analysis.

Table 2 Partial safety factors for stress, flaw size (on mean/best estimate values) and toughness (on characteristic value) for fracture assessments at Level 2

	Partial factors for failure consequences	
Data variable	*Moderate*	*Severe*
Stress (measured), (C.O.V. 5%) γ_s	1.1	1.4
Stress (estimated), (C.O.V. 30%) γ_s	1.2	1.6
Flaw size (S.D. 2–5 mm) γ_a	1.0	1.2
Flaw size (S.D. 10 mm) γ_a	1.1	1.4
Toughness K_{mat} (min 3) γ_t	1.0	1.2
Toughness δ_{mat} (min 3) γ_t	1.0	1.4

Conclusions

The assessment of defects in complex problems of welded joints can be reduced to separate consideration of linear elastic stress intensity factors, and plastic collapse solutions, provided the assessment diagram used is appropriate for the materials and geometries concerned. In effect the assessment diagram is a means of allowing for the enhancement of crack tip driving force by plasticity, whilst the user only has to estimate linear elastic stress intensity factor values which can be done by parametric formulae and magnification factors for complex geometries.

In fillet welds and tubular joints, consideration has to be given to failure either through the weld or from the weld toe, and to the effects of defects at each of these locations. These magnification factors can then also be applied to fracture or fatigue calculations. Three dimensional elastic–plastic fracture mechanics methods now offer the promise of modelling cracked complex geometries and defining where the standard assessment diagrams are adequate or require modification. These analyses are still much too expensive for normal application and hence standardised procedures are necessary such as the assessment diagram approach. Confirmation of overall geometry behaviour by model testing represents a powerful support to the finite element analysis.

It is also necessary to make adequate allowance for variability in input data for defect assessment, and methods to achieve this via reliability analysis are now available.

Appendix 1

M_k *equations:* $M_k = p(a/T)^q$

Tension peak path

$0.008 < a/T \leqslant 0.1$

$$p = 1.2375(L/T)^{-0.01446}(R/T)^{0.1225}\{1 - 0.27(\theta) - 0.0575(\theta)^2\}$$

$$q = -0.013(L/T)^{0.0675}(R/T)^{-0.347}\{1 + 7.71(\theta) - 3.1(\theta)^2\}$$

$0.1 < a/T \leqslant 0.2$

$$p = 0.7801(L/T)^{-0.05}\{1 + 0.14(R/T)\}\{1 + 0.078(\theta) - 0.0625(\theta)^2\}$$

$$q = -0.128(L/T)^{0.085}\{R^{(0.028-0.88(R/T))}\}\{1 - 0.687\theta + 1.9(\theta)^2 - 0.88(\theta)^3\}$$

Pure bending peak path

$0.008 < a/T \leqslant 0.15$

$$p = 1.06(L/T)^{0.0458}(R/T)^{0.1138}\{1 - 0.541(\theta) + 0.197(\theta)^2\}$$

$$q = -0.046(L/T)^{0.0269}(R/T)^{-0.237}\{1 + 2.892(\theta) - 1.034(\theta)^2\}$$

Validity ranges

a/T – *as specified*

$0.75 \leqslant L/T \leqslant 2.0$

$22.5 \leqslant \theta \leqslant 90$ degrees

$0.01 \leqslant R/T \leqslant 0.5$

Acknowledgements

The SHS materials and welded samples were generously provided by Robert Watson (Constructional Engineers) Ltd, Bolton to whom grateful acknowledgement is made.

References

(1) BSI Document PD6493 (1980).
(2) HARRISON, R. P., LOOSEMORE, K., and MILNE, I. (1976–80) Assessment of the integrity of structures containing defects, CEGB Reports R/H/R6, 1976; Revision **1** – 1977; Revision **2** – 1980.
(3) MILNE, I., AINSWORTH, R. A., DOWLING, A. R., and STEWART, T. (1986) CEGB Report R/H/R6, Revision **3**.
(4) MILNE, I., AINSWORTH, R. A., DOWLING, A. R., and STEWART, A. T. (1987) Background to and validation of CEGB Report R/H/R6 Revision 3, R/H/R6 Revision 3 Validation.
(5) Revised version of BSI Document PD 6493 (1991) in press. See also Burdekin, F. M., Garwood, S. J., and Milne, I. (1988), The basis for the technical revisions to the fracture clauses of PD 6493, *International Conference on Weld Failures*, Welding Institute, Cambridge, Paper 37.
(6) FISHER, J. W. and FRANK, A. (1979) *ASCE, J. Structural Division*, **105**, 1727–1740.
(7) SAKET, H. K. (1988) *The fatigue behaviour of fillet welded joints of plates and square hollow sections*, PhD Thesis, UMIST.
(8) MADDOX, S. J. (1975) An analysis of fatigue cracks in fillet welded joints, *Int. J. Fracture*, **11**, 221–243.
(9) AHMET, M. T. (1980) *The effect of thickness on allowable defect sizes in fillet welded joints under fatigue loading*, MSc Thesis, UMIST.
(10) LIE, S. T. (1983) *The influence of geometrical parameters on the fatigue strength of fillet welds using boundary element and fracture mechanics methods*, PhD Thesis, UMIST.
(11) ALBRECHT, P. and YAMADA, K. (1977) *ASCE, J. Structural Division*, **103**, 377–389.
(12) BURDEKIN, F. M., CHU, W. H., CHAN, W. T. W., and MANTEGHI, S. (1986) Fracture mechanics analysis of crack propagation in tubular joints, *Fatigue and crack growth in offshore structures*, IMechE, London, pp. 31–48.
(13) BURDEKIN, F. M., CHAN, W. T. W., MANTEGHI, S., and THURLBECK, S. D. (1988) *Fatigue of Offshore Structures*, (Edited by W. D. Dover and G. Glinka), EMAS, Warley.
(14) BEALE, L. A. and TOPRAC, A. A. (1967) Structures Fatigue Research Laboratory Report, University of Texas, Austin, TX.
(15) UEG Publication UR33 (1985) Design of tubular joints for offshore structures, UEG/CIRIA, London.
(16) LALANI, M., GHOLKAR, S. F., and WARD, J. K. (1989) OTC 21st Annual Conf., Vol. 4, Paper OTC 6158.
(17) PLANE, C., COWLING, M. J., NWEGBU, V. K., and BURDEKIN, F. M. (1987) *Integrity of Offshore Structures, IOS-3*, (Edited by Faulkner, O. *et al.*), Elsevier Applied Science, London.